



A Simple Thermal Decomposition Method for Synthesis of $\text{Co}_{0.6}\text{Zn}_{0.4}\text{Fe}_2\text{O}_4$ Magnetic Nanoparticles

Ibrahim Sharifi¹, Ali Zamanian^{*1}, Aliasghar Behnamghader¹

¹Nanotechnology and Advance Materials Department, Materials and Energy Research Center (MERC), P.O. Box 31787-316, Karaj, Iran.

Received: 14 January 2016; Accepted: 15 June 2016

Corresponding author email: a-zamanian@merc.ac.ir

ABSTRACT

Magnetic nanoparticles attracted a great deal of attention in the medical applications due to their unique properties. The most exceptional property of magnetic particles is their response to a magnetic force, and this property has been utilized in applications such as drug targeting, bioseparation, contrast agents in magnetic resonance imaging (MRI) and heating mediators for cancer therapy. In this study, a ternary system of $\text{Co}_{0.4}\text{Zn}_{0.6}\text{Fe}_2\text{O}_4$ was synthesized by thermal decomposition method using metal acetylacetonate in high temperature boiling point solvent and fatty acids. Unlike other synthesis techniques this method can be get nearly monodispersed nanoparticles that makes them suitable for medical applications like hyperthermia. X-ray diffraction study was used to determine phase purity, crystal structure, and average crystallite size of cobalt-zinc ferrite nanoparticles. The average diameter of particles was determined by field emission scanning electron microscope (FESEM) around 16 nm. Fourier transform infrared (FT-IR) measurement confirmed mono phase spinel structure of ferrite. The as-prepared ferrite nanoparticles were characterized extensively by other analytic techniques like vibrating sample magnetometer (VSM) to achieve magnetic properties of nanoparticles. Room temperature magnetization measurements showed the magnetization M_s and coercivity of magnetic nanoparticles as high as 74 emu/g and 114 Oe, which can be a good candidate for use in hyperthermia applications.

Keywords: Ferrite nano particles; Thermal decomposition; Cobalt-Zinc; Rietveld refinement method.

How to cite this article:

Sharifi I, Zamanian A, Behnamghader A. A Simple Thermal Decomposition Method for Synthesis of $\text{Co}_{0.6}\text{Zn}_{0.4}\text{Fe}_2\text{O}_4$ Magnetic Nanoparticles. *J Ultrafine Grained Nanostruct Mater*, 2016; 49(2):87-91.

DOI: [10.7508/jufgsm.2016.02.05](https://doi.org/10.7508/jufgsm.2016.02.05)

1. Introduction

In the last decade, nanotechnology has developed to such an extent that it has become possible to fabricate, characterize and specially tailor the functional properties of nanoparticles for biomedical applications such as cancer treatment by hyperthermia [1], MRI contrast agent [2], drug delivery [3] and cell separation [4]. For these applications, the particles must have

combined properties of high magnetic saturation, biocompatibility and interactive functions at the surface [5].

Due to the ease of preparation, together with their good magnetic properties, Fe_3O_4 and CoFe_2O_4 are the preferred and best characterized materials among magnetic nanoparticle materials. Fe_3O_4 and CoFe_2O_4 nanoparticles both possess a high saturation magnetization, and good chemical

stability. Both particle species have similar densities, crystal structures and magnetization.

Magnetic hyperthermia is strictly related to heat dissipation from different loss mechanism in magnetic materials. The mechanism of losses in the magnetic particles can be different by changing the size of magnetic nanoparticles. When the particle size is between single domain and superparamagnetic state, there is an existence of three type of magnetic loss mechanism included hysteresis loss, Brownian and Néel relaxation losses. Cobalt ferrite has a higher magnetic anisotropy, so that it was expected to have a greater hysteresis loop in compare of magnetite. When a magnetic particle exposed to an alternating magnetic field, with a delay in the relaxation of the magnetic moment through either the rotation within the particle (Néel) or the rotation of the particle itself (Brownian), heat dissipation can be occurred. Néel relaxation has a straight relationship with magnetic anisotropy, so that; $\tau_N = \tau_0 \exp(KV_M/k_B T)$ where τ_N is the Néel relaxation time, $\tau_0 = 10^{-9}$ s, K the anisotropy constant, V_M the volume of particle, k_B the Boltzmann constant, T the temperature [1].

So that, by the use of cobalt ferrite with higher magnetic anisotropy, the effectiveness of heat dissipation enhanced. Also, by doping 0.4 Zn^{2+} instead of Co^{2+} in the structure of $Co^{2+}Fe^{3+}_2O_4$, saturation magnetization (M_s) of magnetic nanoparticles placed in the maximized state [6].

So that, in this article, firstly we synthesized monodisperse magnetic nanoparticles by an easy and economical thermal decomposition route after that, we investigated magnetic properties and structural analysis of modified magnetic nanoparticles.

2. Experimental method

2.1. Materials

Iron(III) acetylacetonate ($Fe(acac)_3$), zinc acetylacetonate ($Zn(acac)_2$), cobalt(II) acetylacetonate ($Co(acac)_2$), were acquired from E. Merck Co. Germany and other contents such as Oleic acid and Benzyl ether obtained from Sigma Aldrich Co., USA and all of them used as they received without further treating.

2.2. Synthesis

Synthesis was carried out under a nitrogen atmosphere using standard Schlenk line techniques. Magnetic nanoparticles were first synthesized in the presence of oleic acid and benzyl ether.

For synthesis of $Co_{0.6}Zn_{0.4}Fe_2O_4$ nanoparticles we have adopted a method, which is based on thermal decomposition of acetylacetonate precursors. In a typical experiment for synthesis of Co-Zn ferrite, Fe(III) acetylacetonate (0.71 g, 2.00 mmol), Co(II) acetylacetonate (0.15 g, 0.60 mmol), Zn(II) acetylacetonate (0.11 g, 0.40 mmol), oleic acid (1.7 mL, 4.00 mmol), and benzyl ether (30 mL) were heated together until 110 °C and degassed at this temperature for 1 h. The solution was then heated to the reflux temperature (~320 °C) of the solution at the rate of 20 °C/min with vigorous magnetic stirring. The reaction mixture was kept at this temperature for 30 minutes. After refluxing, the solution was cooled to the room temperature, and a mixture of toluene (40 ml) and hexane (10 ml) was added to the solution. By using the magnetic decantation technique magnetic nanoparticles was separated and after washed three times with a mixture of chloroform/methane, it was redispersed in chloroform (or left to dry overnight for the case of the magnetic and structural characterization measurements).

2.3. Characterization

X-Ray powder diffraction patterns were recorded on a Philips X-ray diffractometer with $Co-K_\alpha$ radiation ($\lambda = 1.78901$ Å). The scans of the selected diffraction peaks were carried out in step mode (step size 0.02°, measurement time 2s, measurement temperature 25 °C, and standard: Si powder). SEM study was carried out in a TESCAN field emission type scanning electron microscope at 10 kV. Average particle size and size distribution were determined through post-processing of the FESEM images with SemAfore software. The Fourier Transform Infrared Spectroscopy (FTIR) in far spectrum was recorded as (KBr) discs in the range 4000–400 cm^{-1} by using the (Perkin Elmer FTIR, 1403, USA) spectrophotometer. The magnetic measurements of the prepared powder were determined at room temperature by using the vibrating sample magnetometer (VSM) (Meghnatis Daghigh Kavir Co., Kashan, Iran).

3. Results and discussion

3.1. Chemical analysis and scanning electron microscopy

The thermal decomposition processing of organometallic precursors led to the synthesis of homogeneous $Co_{0.6}Zn_{0.4}Fe_2O_4$ nanoparticles. The XRD profile of samples confirmed the presence

of ferrite with spinel structure. For obtaining the correct value of crystallite size and lattice parameter X-ray diffraction patterns were processed by using the computer Program Materials Studio in the Rietveld method. Rietveld refinement of the samples was done with experimental diffraction patterns of ferrite nanoparticles and crystallography information file of cobalt ferrite structures that substituted by zinc ions instead of cobalt ions in the stoichiometry value. Fig. 1 shows the X-ray diffraction patterns of the Cobalt-Zinc ferrite that was processed by Rietveld refinement method. The positions and relative intensities of all the diffraction peaks match well with the Co-Zn ferrite profiles. The peaks that be indexed at the values of 2θ in XRD patterns in 21.4° , 34.9° , 41.1° , 43.4° , 50.3° , 62.6° , 67.0° , and 73.9° corresponding to the crystal planes of (111), (220), (311), (222), (400), (422), (511) and (440), respectively. The strong peaks with minimal background noise in XRD patterns obviously indicate the formation of fully

crystalline ferrite spinel structure with space group symmetry $fd\bar{3}m$. Also, the reflections are reasonably broader, revealing the nano-size of the crystals. It is not seen any impurity peaks in the XRD patterns of the particles, as a result of indicative of the high purity of the ferrite nanoparticles.

The calculated lattice parameter from these diffraction peaks is 8.407 \AA , which is slightly smaller than the known to the $\text{Co}_{0.6}\text{Zn}_{0.4}\text{Fe}_2\text{O}_4$ (8.428 \AA) as observed by Jnaneshwara et al [7] that was prepared by the solution combustion method, and also this lattice parameter is larger than the value (8.383 \AA) that was reported by Arulmurugan which as-synthesized Co-Zn ferrite prepared by co-precipitation method [8]. The crystallite mean size was achieved by a Rietveld refinement method for the Co-Zn ferrite sample, obtaining 15 nm.

The FESEM micrograph of the Co-Zn ferrite nanoparticles is illustrated in Fig. 2-a As can be seen the sample contains uniformly distributed spherical nanoparticles. Also, Fig.2-b shows size distribution

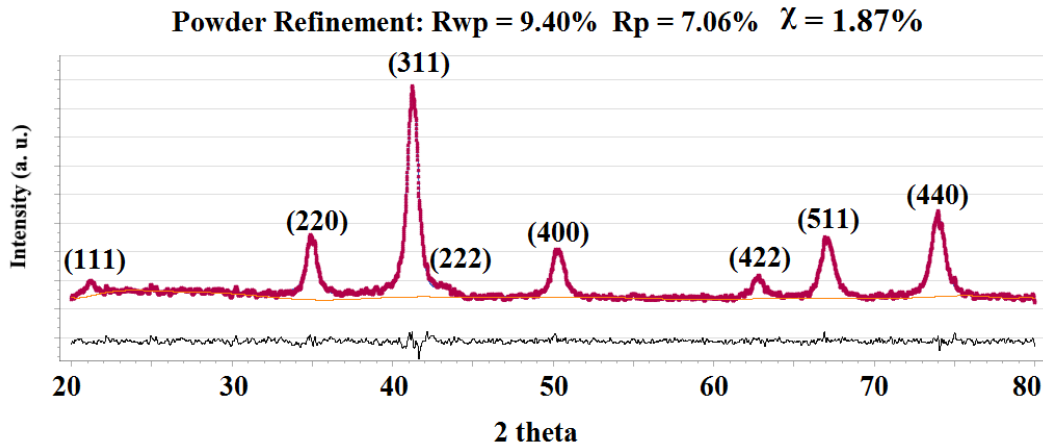


Fig. 1- X-Ray powder diffraction patterns of Co-Zn Ferrite nanoparticles.

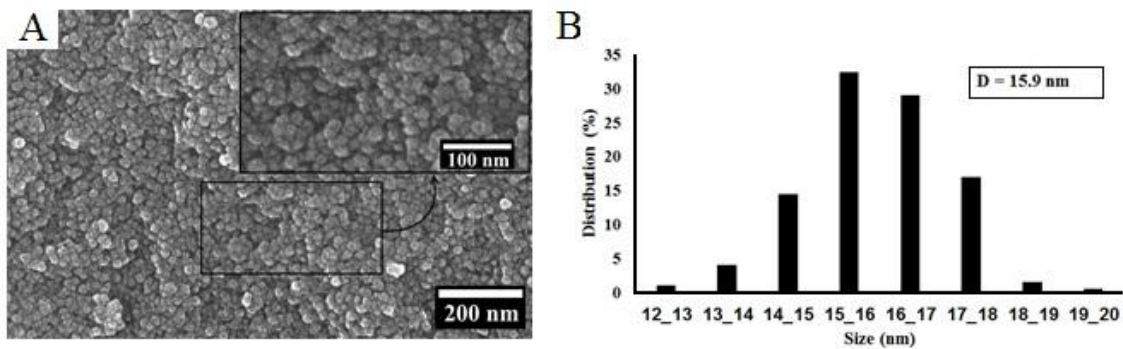


Fig. 2- a) FESEM image of as-synthesized magnetic nanoparticles, b) average particle size and size distribution.

of nanoparticles. Mean size of nanoparticles is about 15.9 nm. This value is in close agreement with the average crystallite size obtained from the X-Ray powder diffraction patterns by using the Rietveld refinement for the ferrite sample.

To provide further evidence about the structure of the Fe-Zn ferrites, the samples were characterized by FTIR spectroscopy (Fig. 3). The FTIR spectra of the magnetic nanoparticles show a strong band (ν_1) around 578 cm^{-1} as a result of Metal-O stretching vibrations of the tetrahedral site, and a weak band (ν_2) around 418 cm^{-1} due to octahedral metal stretching of spinel structure [9].

3.2. Magnetic hysteretic properties

Hysteresis loops plotted from the VSM measurements are given in Fig. 4. The as-synthesized Co-Zn ferrite nanoparticles showed ferromagnetic behaviours at the room temperature (300 K) with a small coercivity (H_c) of 114 Oe (Fig. 2) and remanence magnetization (M_r) of 12.8 emu/g. At 300 K the saturation magnetization (M_s) of these magnetic nanoparticles was 74.5 emu/g, which is higher than that of cobalt ferrite nanoparticles in similar size. It is probably because zinc can be changed cation distribution of cobalt and iron ions in different spinel sites. Also, with respect to that zinc has a larger ions size, it can be caused to change the size of the octahedral and tetrahedral site in the spinel structure. So that, the exchange force between the moments of different sites has been changed as a result of changing the angle and distances among ions and the oxygen ion that links them together [10].

4. Conclusion

In summary, High quality magnetic nanoparticles with average sizes 16 nm were synthesized by a simple thermal decomposition

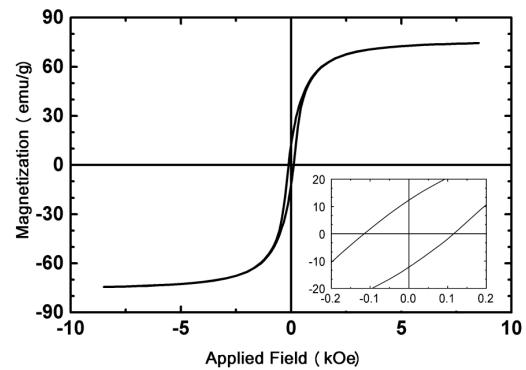


Fig. 4- Magnetization curve versus applied field at 300 K for Co-Zn ferrite nanoparticles.

method. The study showed that, as-synthesized nanoparticles has a good magnetic properties with high saturation magnetization as high as 74 emu/g. Also, with respect to FESEM micrograph size distribution of nanoparticles was so narrow. So that, magnetic nanoparticles will be applicable as the basic unit to magnetic hyperthermia.

References

1. Sharifi I, Shokrollahi H, Amiri S. Ferrite-based magnetic nanofluids used in hyperthermia applications. *Journal of Magnetism and Magnetic Materials*. 2012;324(6):903-15.
2. Pouponneau P, Leroux JC, Soulez G, Gaboury L, Martel S. Co-encapsulation of magnetic nanoparticles and doxorubicin into biodegradable microcarriers for deep tissue targeting by vascular MRI navigation. *Biomaterials*. 2011;32(13):3481-6.
3. Veisheh O, Gunn JW, Zhang M. Design and fabrication of magnetic nanoparticles for targeted drug delivery and imaging. *Advanced Drug Delivery Reviews*. 2010;62(3):284-304.
4. Xu H, Aguilar ZP, Yang L, Kuang M, Duan H, Xiong Y, Wei H, Wang A. Antibody conjugated magnetic iron oxide nanoparticles for cancer cell separation in fresh whole blood. *Biomaterials*. 2011;32(36):9758-65.
5. Gupta AK, Gupta M. Synthesis and surface engineering of iron oxide nanoparticles for biomedical applications. *Biomaterials*. 2005;26(18):3995-4021.
6. Yoo D, Lee JH, Shin TH, Cheon J. Theranostic magnetic

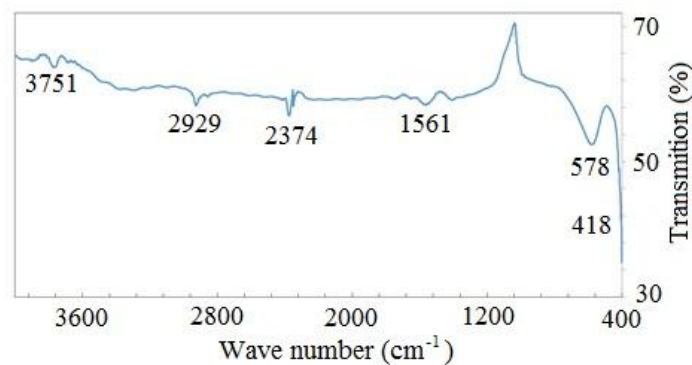


Fig. 3- The FTIR spectra of Co-Zn ferrite nanoparticles.

- nanoparticles. *Accounts of Chemical Research*. 2011;44(10):863-74.
7. Jnaneshwara DM, Avadhani DN, Prasad BD, Nagabhushana BM, Nagabhushana H, Sharma SC, Prashantha SC, Shivakumara C. Effect of zinc substitution on the nanocobalt ferrite powders for nanoelectronic devices. *Journal of Alloys and Compounds*. 2014;587:50-8.
8. Arulmurugan R, Jeyadevan B, Vaidyanathan G, Sendhilnathan S. Effect of zinc substitution on Co-Zn and Mn-Zn ferrite nanoparticles prepared by co-precipitation. *Journal of Magnetism and Magnetic Materials*. 2005;288:470-7.
9. Praveena K, Sadhana K. Ferromagnetic Properties of Zn substituted Spinel Ferrites for High Frequency Applications. *International Journal of Scientific and Research Publications*. 2015;5(4):1-21.
10. Goldman A. Chemical aspects of ferrites. *Modern Ferrite Technology*. 2006:71-110.